Accurate Characterization of Planar Printed Antennas Using Finite-Difference Time-Domain Method

Chen Wu, *Member, IEEE,* Ke-Li Wu, *Member, IEEE,* Zhi-Qiang Bi, *Student Member, IEEE,* and John Litva, *Member, IEEE*

Abstract—**The finite-difference time-domain method (FDTD) is used to accurately characterize complex planar printed antennas with various feed structures, which include coaxial probe feed, microstrip line feed, and aperture coupled feed structures. A new coaxial probe model is developed by using a three-dimensional FDTD technique. This model is shown to be an efficient and accurate tool for modeling coaxial-line fed structures. A novel use of a dispersive absorbing boundary condition is presented for a printed antenna with a high dielectric constant. All the numerical results obtained by the FDTD method are compared with experimental results, and the comparison shows excellent agreement over a wide frequency band.**

I. Introduction

THE popularity of planar printed antennas has steadily increased over the past decade, or so, due to a number of advantages such as low cost, low weight, low profile, conformability with existing structures, and ease of fabrication and integration with active devices. During this time they have become an important area of activity within the antenna community and have led to a major innovation in antenna theory. Usually, printed antennas are fabricated on a substrate, or on a number of substrates backed by a metallic sheet (the ground plane). The radiating elements, consisting of thin metallic patches or slots in a metallic sheet, are located at an interface, commonly consisting of a dielectric and air. Multilayered or stacked structures are often used to increase antenna bandwidth. This can be achieved, for example, by simply introducing an air gap between the dielectric layers. Usually, the bandwidth can be increased to more than 10%. Practically, there are three common structures that are used to feed planar printed antennas. These are coaxial probe feeds, microstrip line feeds, and aperture-coupled feeds. The coaxial-fed structure is often used in a single element or a small array because of the ease of matching its characteristic impedance to that of the antenna; and, as well as, the parasitic radiation from the feed network tends to be insignificant. Furthermore, it can also be used as the transition from a printed circuit located on one side of a substrate to the printed antenna on the other side. Compared to probe feeds, microstrip line-fed structures are more suitable for larger arrays due to the ease of fabrication and lower costs, but the serious drawback of this feed structure is the strong parasitic radiation [1]. The aperture-coupled structure has all of the advantages of the former two structures, and isolates the radiation from the feed network, thereby leaving the main antenna radiation uncontaminated. All three of these practical feed structures will be discussed in this paper.

To date, many numerical techniques [1]–[6] have been developed to analyze planar printed antennas in the spectral domain. For coaxial-fed patch antennas, the earliest model to be adopted for full wave analysis is the delta current source model [2]. The model is based on the use of sinusoidal expansion modes and the assumption that the current on the probe is constant. The assumption restricts the model to the point where reasonable results can be obtained only near the resonant frequency of the patch antenna. Another popular model is based on sophisticated attachment models [3], in which the excitation current was spread over a charge cell. This model was developed to be compatible with the rooftop basis functions. Unfortunately, the resulting matrix needs to be carefully treated because it is severely ill conditioned in the vicinity of the resonant frequency. Recently, a more accurate spectral domain model was developed [4], in which the fringing field is replaced by a frill of magnetic current. However, the discontinuity between the coaxial line and the patch substrate, as well as the higher mode near the connector region, cannot be easily accounted for, even though a primary transverse electromagnetic (TEM) mode excitation concept is incorporated in the model. It is found that the spectral domain methods can provide a more accurate model for microstrip line-fed antennas than that for coaxial-fed antennas, even though some non-practical assumptions must be imposed in the line-fed model. A number of assumptions, such as the transverse directed currents [5] are not being taken into account and little consideration being given to contributions from higher modes propagating down the feed line, will cause the numerical results to diverge as the frequency increase. Furthermore, when a antenna consists of a multilayered structure, the spectral domain methods become more difficult to use because of the complexity of the Sommerfeld-type integral treatment.

The finite-difference time-domain (FDTD) method has been

Manuscript received September 20, 1991; revised January 2, 1992. This work was supported by the Telecommunication Research Institute of Canada (TRIO).

The authors are with the Communications Research Laboratory, McMaster University, Hamilton, ON Canada L8S 4K1.

IEEE Log Number 9200365.

widely used to solve electromagnetic problems since 1966. Because Maxwell's equation are discretized directly, using central difference in both space and time, the FDTD method is more flexible for modeling complex structures. In the last few years, a number of investigators have used the FDTD method to analyze microstrip problems [7]–[9], but in the case of the coaxial-line feed problem the analysis is based on assumptions that deviate from practice. For example, the discontinuity between the coaxial line and patch region is replaced by an equivalent lump resistance, and as well, the characteristic impedance of the coaxial line is not included in the model [7]. Obviously, it is very difficult to obtain an accurate equivalent resistance to incorporate all of the effects of the discontinuity near the connector, especially if the modeling is being carried out over a wide frequency range. On the other hand, although a number of researchers have given attention to modeling line-fed printed antennas using the FDTD method, as of yet, none has addressed the problem of strong dispersion when the dielectric constant is high. This situation will be addressed here using a dispersive absorbing boundary condition.

In this paper it will be shown that the FDTD method provides a technique for accurate modeling of planar printed antennas. There are three features of this full-wave analysis technique that will be highlighted. First, rather than being limited to a treatment of simple printed antenna structures, this study focuses on various complex printed antennas, such as coaxial-fed stacked microstrip antennas, microstrip line-fed aperture coupled stacked microstrip antennas, and printed slot antennas. Second, a new coaxial feed model is presented, which provides a robust description of probe feeds, as well as allowing for modeling of complex printed antennas. The model takes into account contributions from the higher order modes at the junction between the probe and the antenna. The validity of the model is demonstrated by a comparison of simulated and experimental results. The example, which will be discussed in detail, is the coax-to-microstrip transition. This problem often occurs in practical printed antenna designs. The third feature of this paper is the novel use of a dispersive absorbing condition. Its implementation will be shown to be quite straightforward. This boundary condition is useful in analyzing printed antenna structures which contain microstrip lines, where the dielectric constant of the substrate is high.

The antenna structures that are analyzed in this paper can be considered to be representative of printed antenna structures. Also, the results of the sophisticated numerical treatment will be shown to be in excellent agreement with the experimental results over a very wide frequency range, the experimental results that are used to validate the numerical modeling were obtained using the HP8510B network analyzer. Details with regard to calibration and measurement error will be provided in the following sections.

II. Numerical Implementations and Experimental Considerations

The FDTD method is formulated using a central difference discretization of Maxwell's curl equations in both time and space. Yee's original algorithm [10] solving Maxwell's equations in three dimension is adopted. The field values on the nodal points of the discretized finite volume are calculated in a leapfrog fashion. In order to enhance the capabilities of the FDTD method with planar antennas, two major developments are used in conjunction with the algorithm. The first is a coaxial feed model and the second is the dispersive boundary condition.

A. Leapfrog Algorithm

Since the FDTD algorithm is well known, only the fundamentals of its operation will be described here. For simplicity, the antenna substrates will be assumed to be isotropic, homogeneous and lossless. With these assumptions, Maxwell's curl equations can be expressed as

$$\mu \frac{\partial \mathbf{H}}{\partial t} = -\nabla \times \mathbf{E} \tag{1}$$

$$\epsilon \frac{\partial \mathbf{E}}{\partial t} = \nabla \times \mathbf{H} \tag{2}$$

and may be discretized by using the central difference scheme. The central difference technique reduces the round-off error for accuracy to the second-order. With time and space discretized, the **E**- and **H**-fields are interlaced within the spatial 3-D grid. All of these points are brought to light by the leapfrog formula; a representative sample of which is given by

$$\begin{aligned} E_x^{n+1}(i,j,k) &= E_x^n(i,j,k) + \frac{\Delta t}{\epsilon} \cdot \left[\frac{H_z^{n+1/2}(i,j+1,k) - H_z^{n-1/2}(i,j,k)}{\Delta y} \right. \\ &\quad \left. - \frac{H_y^{n+1/2}(i,j,k+1) - H_y^{n-1/2}(i,j,k)}{\Delta z} \right]. \end{aligned} \tag{3}$$

The time step in (3) must be limited by the stability criterion

$$\Delta t \le \frac{1}{v_{\max} \sqrt{\frac{1}{\Delta x^2} + \frac{1}{\Delta y^2} + \frac{1}{\Delta z^2}}} \tag{4}$$

where Δx, Δy, and Δz are the space steps in the x-, y-, and z-directions. The quantity, Δt, is the time step and $v_{\max}$ is the maximum velocity in the computational domain.

At this point, Maxwell's equations have been replaced by a system of computer recognizable finite-difference equations. The leapfrog algorithm is able to start working as soon as the boundary conditions are set up. The excitation plane is a special component of the boundary plane, which needs to be treated carefully when setting up the problem.

B. Excitation Treatment

For planar printed antenna problems, microstrip lines and coaxial probes are the basic structures used as feeds. It is assumed that the fields in the computational domain are identically zero at time $t = 0$. The Gaussian pulse is used as

the source of excitation because its smooth Gaussian shaped spectrum can provide information from dc to the desired frequency simply by adjusting the width of the pulse.

In the case of microstrip line or microstrip line-fed problems, the electric or magnetic wall condition is used at the front plane of the device, i.e., at the point at which the wave is launched. An impulse of vertical electric field is applied underneath the microstrip line as the excitation. It is a plane in the spatial domain and has a Gaussian shape in the time domain. Although a fictitious source is used, the boundary conditions will force the field to take on a realistic distribution after the wave propagates a distance of a few lattices. Once the Gaussian pulse is well clear of the front plane, the front plane is shifted forward a few lattices and is transformed into an absorbing boundary. Because the dominant mode for the microstrip line is the *quasi*-TEM mode, which is known to be dispersive, the dispersive characteristics of the waves propagating on the line must be taken into account by using dispersive absorbing condition. This becomes more important when the dielectric constant of the substrate is very high, for example $\epsilon_r = 10.2$.

From a knowledge of the modes that exist on a coaxial line, a simple field distribution can be specified at the excitation plane, i.e., the plane between the feed and the antenna, in such a way that the field components in the rectangular coordinate system take on the projected values of the analytically derived radius-field-distribution. The non-TEM modes that are excited by the nonphysical excitation will decay after propagating at most a few lattices. The only mode which is able to propagate down the coaxial line is the TEM mode. Because the TEM mode is a nondispersive wave, the first-order absorbing boundary will absorb almost all the wave reflected from the antenna to excitation plane of the coaxial line.

C. Coaxial Feed Modeling

The coaxial line-fed connection is a critical part of coaxial-fed patch antennas and needs a special treatment. The curved boundary of the inner and outer conductors of a coaxial line is approximated by staircasing, and the tangential component of the **E**-field is forced to zero at the conductor surface. For the purpose of fitting the numerical coaxial line with the lattice, the numerical characteristic impedance of an SMA connector and its coaxial line is chosen to be about 47.0 Ω over a broad frequency range.

As shown in Fig. 1, the inner conductor of the coaxial line is attached on the patch antenna going through the dielectric substrate, and the outer conductor is connected to the ground plane. In this model, the antenna is divided into two computational regions. One is the coaxial line region and the other is the microstrip components region. The advantage of using two regions is that the electromagnetic field in the coaxial line can be defined by a small matrix, so that the computational space as well as CPU time expended in the coaxial line region is less than 2% of that expended in a single patch antenna region. Although the boundary of the coaxial line is approximated by using staircasing, the extent to which waves are scattered into the coaxial line is largely determined by the

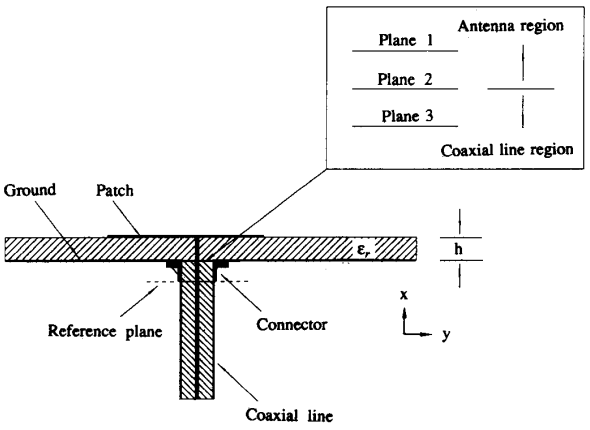

Fig. 1. Side view of a coaxial probe-fed printed antenna.

characteristic impedance of the coaxial line, i.e., its electric characteristics, but seldom upon the specific shape, i.e., its physical characteristics [11]. It is interesting to observe that a very good numerical result can be obtained provided that the numerical characterization impedance of the coaxial line is almost the same as that of the coaxial line used in the measurement.

The two computational regions must be carefully merged near the ground plane. Fig. 1 shows how the two regions are connected. The subscript a and c refer to the field in the antenna and coaxial line regions, respectively. The lattices are the same near the interface plane (plane 2), which is always located on the $E_y - E_z - H_x$ plane in Yee's lattice. Planes 1 and 3 are located at half a lattice immediately above and below plane 2. The E_x, H_y, and H_z components are located on these two planes. The fields in these two computational domains are calculated separately during each time iteration. In the interface region, the **H**-field components can be calculated by the following:

$$\begin{aligned}
h_{xx} &= \left(H_x^{(c)}(i,j,k)_c + H_x^{(a)}(i,j,k)_a\right)/2 \\
H_x^{(c)}(i,j,k)_c &= h_{xx} \\
H_y^{(c)}(i+1,j,k)_c &= H_y^{(a)}(i+1,j,k)_a \\
H_z^{(c)}(i+1,j,k)_c &= H_z^{(a)}(i+1,j,k)_a \\
H_x^{(a)}(i,j,k)_a &= h_{xx} \\
H_y^{(a)}(i,j,k)_a &= H_y^{(c)}(i,j,k)_c \\
H_z^{(a)}(i,j,k)_a &= H_z^{(c)}(i,j,k)_c
\end{aligned} \tag{5}$$

and the **E**-field components by

$$\begin{aligned}
e_{yy} &= \left(E_y^{(c)}(i,j,k)_c + E_y^{(a)}(i,j,k)_a\right)/2 \\
e_{zz} &= \left(E_z^{(c)}(i,j,k)_c + E_z^{(a)}(i,j,k)_a\right)/2 \\
E_x^{(c)}(i+1,j,k)_c &= E_x^{(a)}(i+1,j,k)_a \\
E_y^{(c)}(i,j,k)_c &= e_{yy} \\
E_z^{(c)}(i,j,k)_c &= e_{zz} \\
E_x^{(a)}(i,j,k)_a &= E_x^{(c)}(i,j,k)_c \\
E_y^{(a)}(i,j,k)_a &= e_{yy} \\
E_z^{(a)}(i,j,k)_a &= e_{zz}.
\end{aligned} \tag{6}$$

The two regions are stacked together after the above treatment.

D. Dispersive Boundary Condition

As is well known, a wave traveling down a microstrip line propagates in the waveguide direction. The side wave leakage and radiation are relatively small due to the guiding nature of the metal strip. This is quite similar to a one dimensional propagation problem. Based on the above observations, the first-order boundary condition, i.e.,

$$\left(\frac{\partial}{\partial z} - \frac{1}{v_i}\frac{\partial}{\partial t}\right)E = 0 \tag{7}$$

is usually used, where E represents the tangential electric field components relative to the boundary wall and v_i represents the velocity of propagation of the fields. If this condition is used solely, it is found that the reflections from the boundary can be quite large because the boundary condition only acts as a good absorber at the velocity v_i. Therefore, a dispersive boundary condition which can absorb fields in a wide frequency band needs to be used.

In fact, many wide-angle absorbing boundary condition can be adopted for dispersive problems. For example, it can be seen that the following boundary condition, which was originally developed for wide-angle absorption by Higden [12], can absorb plane waves traveling with velocity v_1 and v_2. The condition is given by

$$\left(\frac{\partial}{\partial z} - \frac{1}{v_1}\frac{\partial}{\partial t}\right)\left(\frac{\partial}{\partial z} - \frac{1}{v_2}\frac{\partial}{\partial t}\right)E = 0. \tag{8}$$

It is easily seen that the above boundary condition is fairly absorptive for any linear combination of plane waves propagating with velocity v_1 and v_2. By concatenating several absorbing boundary conditions, as given by (7), the number of velocities at which absorption is optimized can be increased.

E. Frequency Parameters of Interest

To describe the frequency parameters of planar printed antenna or the properties of the coax-to-microstrip transition, the frequency dependent generalized scattering matrix can be used, which is defined as

$$S_{ij}(f) = \left[\frac{V_i^- \sqrt{Z_{oj}}}{V_j^+ \sqrt{Z_{oi}}}\right]_{V^+_{\text{others}}=0}, \qquad i, j = 1 \text{ or } 2. \tag{9}$$

Ports 1 and 2 represent the coaxial line port of microstrip line port, respectively, and Z_{oi} is the characteristic impedance of the ith port. $V_i^+(f)$ and $V_i^-(f)$ are the incident and reflected voltage waves at the ith port, which are given from the Fourier transform of the voltages in the time domain,

$$V_i^{\pm}(f) = F\{V_i^{\pm}(t)\}. \tag{10}$$

Fig. 2(a) shows a microstrip line-fed rectangular patch antenna with a coax-to-microstrip transition. This problem can be solved by considering the equivalent circuit in Fig. 2(b), where the transition from coax-to-microstrip line is given by a reciprocal lossy two-port network.

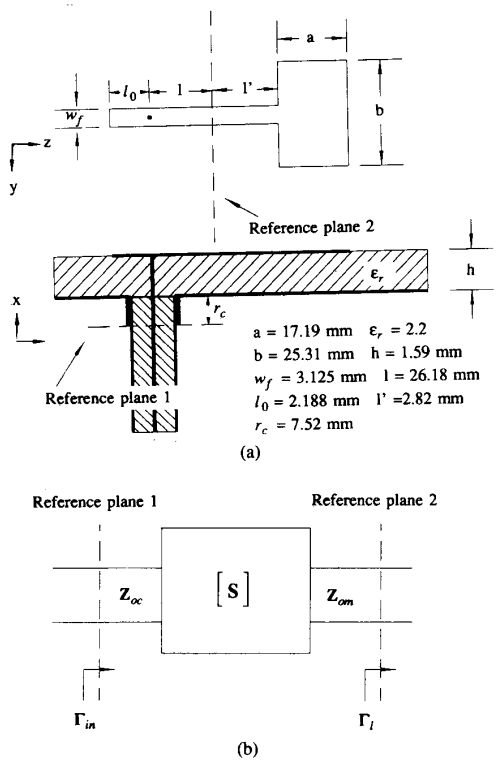

Fig. 2. (a) Microstrip line-fed rectangular patch antenna with coax-to-microstrip transition. (b) Equivalent two-port network of coax-to-microstrip transition.

Reference plane 1 is located in the coaxial line, where the characteristic impedance is Z_{oc}, and Γ_{in} is the reflection coefficient looking into the antenna from plane 1. Once Γ_{in} and $[S]$ for the transition are given, the reflection coefficient Γ_l, which is defined somewhere on the microstrip line can be written as

$$\Gamma_l = \left(S_{22} + \frac{S_{12}S_{21}}{\Gamma_{in} - S_{11}}\right)^{-1}. \tag{11}$$

Simple transmission line theory can then be used if the reference planes need to be shifted along the transmission lines.

Many techniques can be used for deriving the antenna radiation pattern. For example, one can take direct advantage of the FDTD method, because the field at any time step in the computational domain is known during the simulation process. Using an equivalent principle and assuming that the substrate is infinitely large, the air–dielectric interface can be replaced by a conducting sheet on which is superposed a magnetic current. By applying image theory, the surface magnetic current $\mathbf{M}_s$ can be written as

$$\mathbf{M}_s(f) = 2\mathbf{E}(f) \times \mathbf{n} \tag{12}$$

where $\mathbf{E}(f)$ is the electric field on the air–dielectric interface

at a particular frequency and $\mathbf{n}$ is the outward unit vector perpendicular to the interface. After obtaining $\mathbf{M}_s$ and using the free space Green's function of magnetic current, the radiation pattern can be easily obtained.

F. Experimental Considerations

The measurements of the input characteristics of the planar printed antennas under discussion are carried out on an HP8510B network analyzer. To set the reference plane at a specific location, two kinds of calibration techniques are used; one is the standard coaxial line calibration and the other is the TRL calibration. The former can only be used to set the reference plane at the interface between the coaxial-cable and SMA connector (see Fig. 2(a) reference plane 1). The latter can be used to set the reference plane to any place on a line, so that the effect of the coax-to-microstrip transition can be eliminated from the measured results. In the TRL calibration, three calibration kits were required: a Thru line of length l_{thru}, an open-circuit reflect line of length $l_{\text{open}} = l_{\text{thru}}/2$, and a delay line of length $l_{\text{line}} = l_{\text{thru}} + \Delta l$. The resulting reference planes are defined at a distance $l_{\text{thru}}/2$ from the connector to the patch antenna. The characteristic impedance and propagation constant of the three lines must be known for the center frequency and must be the same as those for the line, on which the reference plane is located. Usually $\Delta l = \lambda_g/4$, where λ_g is the waveguide wavelength corresponding to the center frequency in the frequency range of interest. A limitation of the TRL calibration is the fact that only the center-frequency characteristic impedance and propagation constant for the line are used in the calibration. As is well known, the characteristic impedance and effective dielectric constant for a line vary with frequency. The effects of dispersion on the microstrip line can not be taken into account by means of experimental techniques. The limitation brought about by dispersion restricts the bandwith of the measurements, as well as causing measurement errors, especially when the dispersion is serious.

III. Numerical Results and Discussions

To validate the proposed coaxial feed model and to show the improvement that is brought about by using the dispersive boundary condition, four typical complex structures of planar printed antennas are analyzed. These are: a microstrip line-fed rectangular patch antenna with coax-to-microstrip transition, a coaxial-fed stacked patch antenna with an air-gap between two layers, a slot antenna that lies on the ground of a microstrip line, and a microstrip line-fed aperture coupled stacked rectangular patch antenna. Both simulated and measured results will be provided in each case.

With one exception, the first-order absorbing boundary condition (ABC) is used in this study for the top plane, as well as the side walls of the computational domain. The one exception is the strongly dispersive case. In comparison with the higher order ABC, the first-order ABC is considerably simpler to implement. Although a little more computational overhead would be expected. Furthermore, when the lattice size is small compared to the wavelengths of interest, the fields at a boundary are strongly correlated with the fields one lattice inside the boundary. Thus in this case, which is general to the problems being analyzed in this paper, the first-order ABC gives highly accurate and therefore acceptable results.

A. Microstrip Line-Fed Rectangular Patch Antenna with Coax-to-Microstrip Transition

The example shown in Fig. 2(a) consists of two parts. One is a simple patch antenna, which has been studied extensively. The other is a coax-to-microstrip transition. To the best of the authors' knowledge, this transition problem has never been adequately solved over a wide frequency band by any numerical technique, certainly not using analytic analysis. In practice, the transition is widely used in various printed antenna structures, as well as printed circuits. The de-embedding of the effects of the transition is urgently needed for carrying out accurate practical design. In the numerical analysis to follow, reference plane 1 is located at $19\Delta x$ away from the ground plane, and plane 2 is located at $84\Delta z$ from the connector, where $\Delta x = 1.272\Delta h$, $\Delta z = \Delta y = \Delta h = 0.315$ mm. In this example, the microstrip line has a characteristic impedance of 63 Ω at 6 GHz. The first order absorbing boundary condition is applied at a distance of $64\Delta h$ away from the patch. The numerical coaxial line length is $100\,\Delta x$, and the Gaussian pulse is applied at the second grid with respect to the bottom of the coaxial line. The 5% pulse width of the pulse corresponds to 15 space steps with the pulse maximum at $100\,\Delta t$.

The transition from a coaxial line to a microstrip line can be represented by the two-port network shown in Fig. 2(b), and described by S-parameters. Due to the existence of surface and radiation waves, and the fact that only isotropic substrates are considered, the network is lossy, as well as being reciprocal. The S-parameters for this example, calculated by the FDTD method, are shown in Fig. 3. It can be clearly seen that at low frequencies electromagnetic energy is easily transmitted between a coaxial line and a microstrip line. However, at a higher frequency the transmission characteristics degenerate due to the higher order modes at the discontinuity and radiation loss in the microstrip line. It is interesting to note that in this example the energy is seriously blocked at a frequency of around 18 GHz. This blockage is caused mainly by the open end stub, which shorts the circuit at a length of about one quarter of the waveguide wavelength.

The reflection coefficient Γ_{in} of the entire antenna is measured at the reference plane 1, which is located on the coaxial line. Fig. 4 shows the magnitude and phase of Γ_{in} from 3 to 9 GHz (group 1). The measured results are in very good agreement with the calculated results. The reflection coefficient tells us that the antenna is resonant at frequency of 5.53 GHz. The equivalent magnetic current for the air–dielectric interface and at the resonant frequency is given in Fig. 5. In the diagram, the direction and length of each arrow indicates the orientation, phase, and magnitude of the magnetic current at that point. It presents a very clear picture of how the antenna works. At the resonant frequency, the dominant mode on the patch is the fundamental (1, 0) mode. On the two wider edges of the patch, the magnetic current,

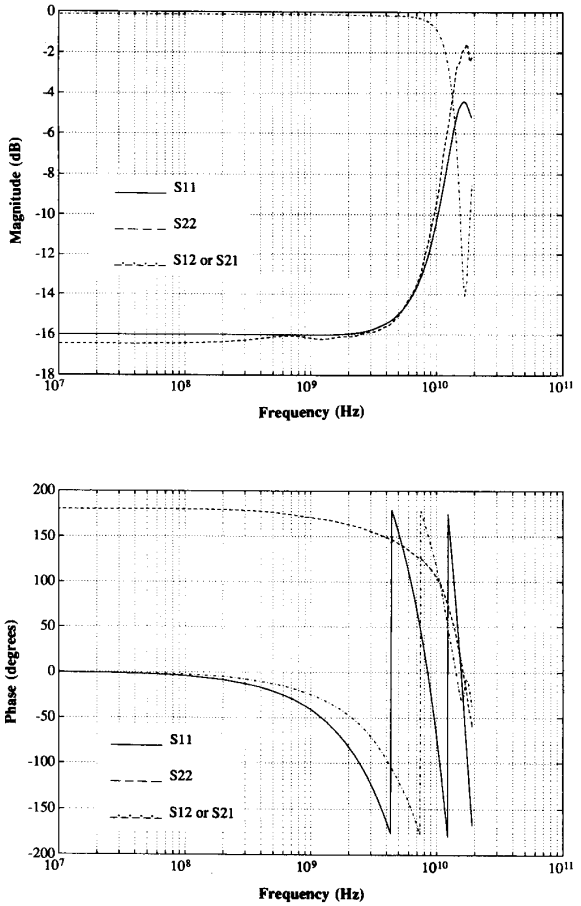

Fig. 3. *S* parameters of coax-to-microstrip transition.

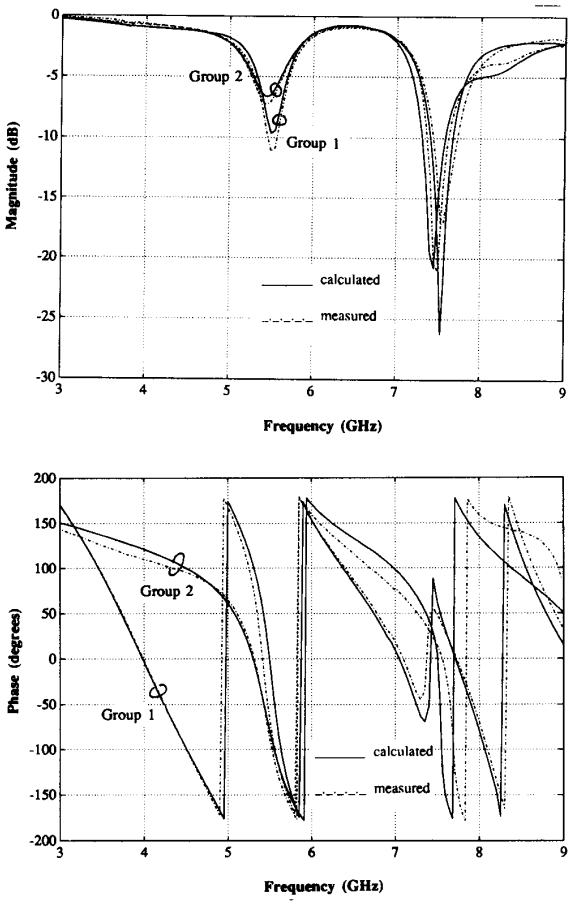

Fig. 4. Reflection coefficients of rectangular patch antenna with coax-to-microstrip transition. Group 1 and Group 2 is defined at reference plane 1 and 2, respectively.

which has almost the same magnitude and phase, contributes mainly to the far field. On the two narrow edges, the current phase changes. The radiation from these currents will almost be cancelled in the far field range.

By using the TRL calibration, the reflection coefficient Γ_l of the patch antenna defined at reference plane 2 (see Fig. 2(a)) is measured and is shown by the dashed line in group 2 of Fig. 4. With the help of (11), the numerical value for Γ_l is obtained by converting Γ_{in}, which is calculated by the FDTD method (see solid line of group 1 in Fig. 4), from reference plane 1 to reference plane 2, using the previously calculated *S*-parameters. It follows from the close agreement that the *S*-parameters of the transition obtained from the FDTD method are correct.

B. Coaxial Probe-Fed Stacked Rectangular Patch Antenna

To show the applicability of the coaxial feed model to more complicated printed antenna structure, the coaxial probe-fed stacked patch antenna is investigated. As shown in Fig. 6, the antenna consists of two patches. The coaxial probe is connected to the lower patch. An air gap is introduced between the two patches in order to increase the

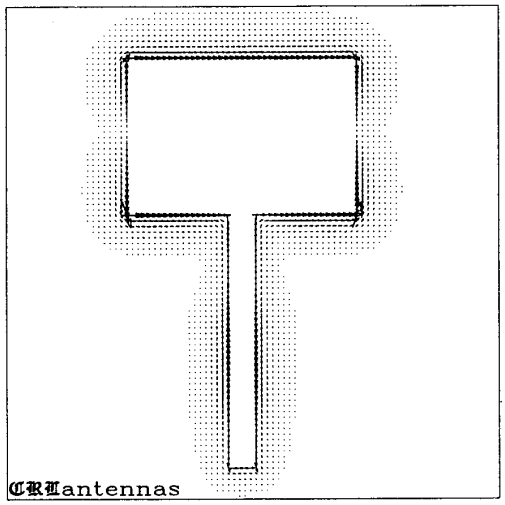

Fig. 5. Magnetic current distribution of the rectangular patch antenna at the interface between air and substrate.

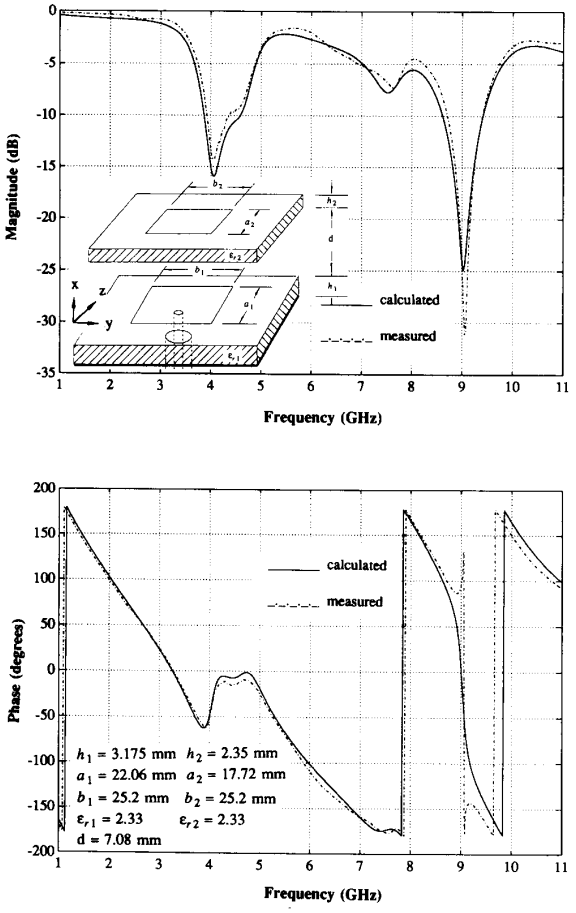

Fig. 6. Reflection coefficient of a coaxial probe-fed stacked patch antenna.

bandwidth of the antenna. In this example, the feed probe is located at a point which is (12.5, 4) mm from the low left corner of the lower patch.

Fig. 6 gives the measured and calculated results for the reflection coefficient of the stacked patch antenna. It is obvious that the comparison is excellent both in magnitude and phase within a wide frequency range. From the reflection coefficient we discover that the antenna has a bandwidth that exceed 16% at the first resonate frequency, within which the return loss is less than -10 dB.

C. Microstrip Line-Fed Slot Antenna

Fig. 7 shows a microstrip line-fed slot antenna, which was analyzed previously in [13] using the spectral domain technique. The computational parameters used in the FD-TD analysis are

$$\Delta h = 0.4 \text{ mm}$$

$$\Delta x = \Delta h, \quad \Delta y = 1.5\Delta h, \quad \Delta z = 1.75\Delta h$$

$$\Delta t = 0.515\Delta h / c$$

and the first-order absorbing boundary is applied. It is assumed that the field across the slot is almost constant; therefore, only one lattice is used.

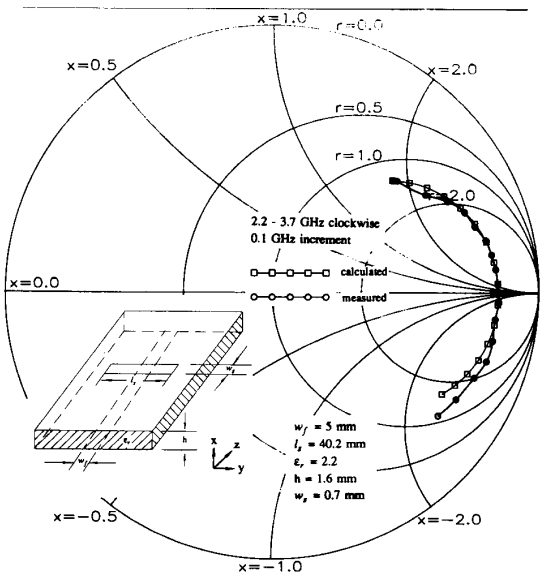

Fig. 7. Input impedance of a microstrip line-fed slot antenna.

The input impedance of the slot antenna in the frequency range from 2.2 to 3.7 GHz is also given in Fig. 7. The reference plane is defined at the center of the slot. The square marks represent the FDTD simulated results and the circular marks give the measured results from [13].

D. Aperture-Coupled Stacked Microstrip Rectangular Patch Antenna

The treatment of the aperture-coupled patch antenna [14] is similar to that of the traditional microstrip antenna except that the microstrip patch antenna is located on one substrate with a relative dielectric constant ϵ_{pr} and a feed network on another substrate with relative dielectric constant ϵ_{fr}. Usually, ϵ_{fr} is higher than ϵ_{pr} in order to reduce the dimensions of the feed network. These two substrates are separated by a common ground plane. In order to couple electromagnetic power from the feed network to the patch antenna, an electrically small opening or aperture is made in the ground plane, as shown in Fig. 8. Since the radiator and the feeder are separated by the common ground plane, the radiation from the feed network can be eliminated from the far-field pattern. As well, the feed network will be decoupled from the antenna. Because ϵ_{fr} usually has a large value, the microstrip line will be strongly dispersive, thereby degrading the performance of the first-order absorbing boundary condition. From numerical experiments in the time domain, it is observed that the reflected wave for a first order boundary is about ten times greater than that from the dispersive absorbing boundary condition discussed in Section II [15]. Therefore, the dispersive boundary condition is used in the analysis to be carried out. In this example, the distance between the open end of microstrip line and the center of the aperture is 3.8 mm. The two velocities that are selected for designing the

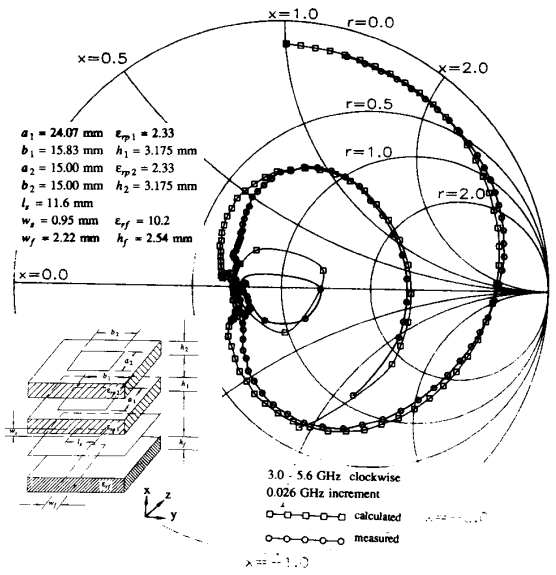

Fig. 8. Input impedance of a aperture-coupled stacked microstrip antenna.

absorbing boundary condition are $v_1 = C/\sqrt{7.12}$ and $v_2 = C/\sqrt{8.5}$. These correspond to frequency 1 and 8 GHz, respectively, where C is the speed of light.

Fig. 8 shows a Smith chart for the input impedance of the aperture coupled stacked patch antenna. Fairly good agreement is observed between calculated and measured results over the frequency band from 3 to 5.6 GHz. This is the band in which the antenna operates most efficiently. Because of the serious dispersion in the microstrip line, it is difficult to design a TRL calibration which is accurate over a wide frequency band. The measurement repeatability of the return loss is about ± 0.05 dB, and phase is about $\pm 8°$. The observed experimental error is primarily due to the uncertainties inherent in the calibration kits that were used for the TRL calibration.

IV. Conclusion

By carrying out a numerical analysis of a number of complex printed antennas, it has been shown that the FDTD method is a very powerful tool for analyzing planar printed antennas. The method can be used to accurately predict all the antenna parameters of interest over a wide frequency range, based on one time-domain simulation. It can provide not only input information for the antennas, but also very detailed field distributions, including the near and far fields. The proposed three-dimensional FDTD coaxial feed model provides a means to address more complicated, but practical printed antenna problems. The validity of the model is demonstrated by comparing the numerical and experimental results for four representative complex antenna structures. A one-dimensional simple dispersive absorbing boundary condition was used when analyzing components of printed antennas with large dielectric constant substrates. In these cases, the wave propagating on the structure suffers serious dispersion. In our experience, the dispersive absorbing boundary can be applied as easily as that of the first order absorbing boundary. The advantage of the dispersive absorbing boundary is that it is defined by the known dispersive characteristics of the transmission line, and it gives second-order performance when the wave propagates in a direction which is normal to the boundary. Finally, it should be noted that advances in the application of the FDTD method to printed antennas require the development of 1) lattices that provide greater numerical efficiency for the analysis of these structures, and 2) the adoption of appropriate signal processing techniques.

Acknowledgment

The authors wish to thank their colleagues, Russ Fralich, for his helpful discussions on this research, and Paul Chung, for help in preparing this manuscript. The authors also wish to thank Sharon R. Aspden of Rogers Corporation for providing the dielectric material used in this research under the auspices of their university program.

References

[1] K. L. Wu, M. Spenuk, J. Litva, and D. G. Fang, "Theoretical and experimental study of feed network effects on the radiation pattern of series-fed microstrip antenna arrays," *Inst. Elec. Eng. Proc.*, pt. H, vol. 138, pp. 238-242, 1991.

[2] D. M. Pozar, "Input impedance and mutual coupling of rectangular microstrip antennas," *IEEE Trans. Antennas Propagat.*, vol. AP-30, pp. 1191-1196, 1982.

[3] J. R. Mosig and F. E. Gardiol, "General integral equation formulation for microstrip antennas and scatterers," *Inst. Elec. Eng. Proc.*, pt. H, vol. 132, pp. 424-432, 1985.

[4] W. C. Chew, Z. Nie, H. Liu, and Y. T. Lo, "Analysis of a probe-fed microstrip disk antenna," *Inst. Elec. Eng. Proc.*, pt. H, vol. 138, pp. 185-191, 1991.

[5] D. M. Pozar and S. M. Voda, "A rigorous analysis of a microstrip line fed patch antenna," *IEEE Trans. Antennas Propagat.*, vol. AP-35, pp. 1343-1349, 1987.

[6] K. L. Wu, J. Litva, R. Fralich, and C. Wu, "Full wave analysis of arbitrarily-shaped line-fed microstrip antennas using triangular finite element method," *Inst. Elec. Eng. Proc.*, pt. H, vol. 138, no. 5, pp. 412-428, 1991.

[7] A. Reineix and B. Jecko, "Analysis of microstrip patch antennas using finite difference time domain method," *IEEE Trans. Antennas Propagat.*, vol. 37, pp. 1361-1368, 1989.

[8] D. M. Sheen, S. M. Ali, M. D. Abouzahra, and J. A. Kong, "Application of the three-dimensional finite-difference time-domain method to the analysis of planar microstrip circuits," *IEEE Trans. Microwave Theory Tech.*, vol. 38, pp. 849-857, 1990.

[9] X. Zhang and K. K. Mei, "Time-domain finite-difference approach to the calculation of the frequency-dependent characteristics of microstrip discontinuities," *IEEE Trans. Microwave Theory Tech.*, vol. 36, pp. 1775-1787, 1988.

[10] K. S. Yee, "Numerical solution of initial boundary value problems involving Maxwell's equations in isotropic media," *IEEE Trans. Antennas Propagat.*, vol. AP-14, pp. 302-307, 1966.

[11] C. Wu, K. L. Wu, Z. Q. Bi, and J. Litva, "Modeling of coaxial-fed microstrip patch antenna by finite difference time domain method," *Electron. Lett.*, vol. 27, no. 19, pp. 1691-1692, 1991.

[12] R. L. Higdon, "Numerical absorbing boundary conditions for the wave equation," *Math. Comput.*, vol. 49, 65-91, 1987.

[13] D. M. Pozar, "A reciprocity method of analysis for printed slot and slot-coupled microstrip antenna," *IEEE Trans. Antennas Propagat.*, vol. AP-34, pp. 1439-1446, 1986.

[14] C. Wu, J. Wang, R. Fralich, and J. Litva, "A rigorous analysis of an aperture-coupled stacked microstrip antenna," *Microwave Opt. Tech. Lett.*, vol. 3, pp. 400-404, 1990.

[15] Z. Q. Bi, K. L. Wu, C. Wu, and J. Litva, "A dispersive boundary condition for microstrip components analysis using FD-TD method," *IEEE Trans. Microwave Theory Tech.*, vol. 40, pp. 774-777, 1992.

Chen Wu (M'90) was born in Beijing, China, on May 2, 1961. He received the B.S. and M.S. degrees in electrical engineering from the East China Normal University, Shanghai, China, in 1983 and 1986, respectively.

From 1986 to 1989 he was a Teaching Assistant and then a Lecturer at the East China Normal University and was engaged in numerical calculations of electromagnetic problems. In 1989, he joined Integrated Antenna Group, Communications Research Laboratory, McMaster University, Hamilton, ON, Canada, as a Research Engineer. He is currently involved in research on integrated antennas, microwave circuits and packaging. He is also interested in numerical modeling and analysis of electromagnetic problems.

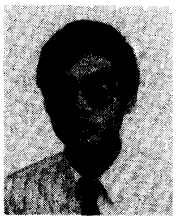

Ke-Li Wu (M'90) was born in Hubei, China, on November 1, 1959. He received the B.S. and M.S.E. degrees from the East China Institute of Technology, Nanjing, China, in 1982 and 1985, respectively, and the Ph.D. degree from Laval University, PQ, Canada, in 1989, all in electrical engineering.

He was a Research Assistant at the East China Institute of Technology, from 1985 to 1986. From 1989 to 1990 he was a Postdoctorate Fellow at McMaster University, Hamilton, ON, Canada. He joined Integrated Antenna Group, Communications Research Laboratory, McMaster University, in 1990 as a Research Engineer. In 1991 he also became an Assistant Professor (part-time) of Electrical and Computer Engineering at McMaster University. His professional interests include all aspects of numerical methods in electromagnetics with emphasis on integrated antennas, microwave circuits, electromagnetic scattering and integrated circuit packaging.

Dr. Wu contributed to *Finite Element and Finite Difference Methods in Electromagnetic Scattering*, Volume 2 of *Progress in Electromagnetics Research* (Elsevier, 1990) and to *Computational Electromagnetics* (North-Holland, 1991).

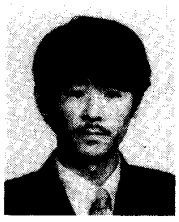

Zhi-Qiang Bi (S'91) was born in Shandong, China, on March 15, 1961. He received the B.S. and M.S.E. degrees from Dalian Maritime University, Dalian, China, in 1982 and 1986, respectively.

He was a Research Assistant from 1982 to 1983, a Teaching Assistant from 1986 to 1988, and a Lecturer from 1988 to 1989 at Dalian Maritime University, where he taught and conducted research in digital signal processing and detection and estimation theories and techniques. Since 1989, he has been a Teaching Assistant, Department of Electrical and Computer Engineering, McMaster University, Hamilton, ON, Canada, where he is working toward the Ph.D. degree. His current research interests include propagation and scattering of electromagnetic waves, design of microwave devices by using numerical and analytical methods, and digital signal processing.

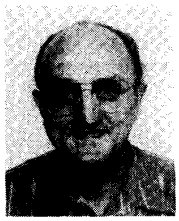

John Litva (M'82) is currently a Professor in Electrical Engineering at McMaster University, Hamilton, ON, Canada, and holds the Microwave Antenna Chair sponsored by Spar Aerospace and Andrew Canada. He is also a thrust leader in the Telecommunications Research Institute of Ontario (TRIO). TRIO is a university-industry based Centre of Excellence, which is funded by the Province of Ontario, and whose mandate is to conduct research in support of the telecommunications industry in Ontario. Prior to 1985 he was a Research Scientist in the Radar Laboratory at the Communications Research Centre, Ottawa, where his primary area of research was low-angle radar tracking of sea skimming missiles. His current research interests center on low-angle radar tracking (matched field processing), scattering theory, radio-wave direction finding, and phased-array antenna theory.